

Compression Strength of Composite Suspension Push-rods for Formula 1 Racing Cars

L. Curley, J. Mallon and M. D. Gilchrist (corresponding author)

Mechanical Engineering Department, University College Dublin, Belfield, Dublin 4, Ireland

ABSTRACT: Advanced composite materials are extensively used in the construction of a contemporary Formula 1 racing car. This paper describes the manufacture and ultimate mechanical performance under compression of composite suspension push-rods that could typically be used in a Grand Prix racing car. An aerofoil-type cross-section was used with different lay-ups of unidirectional and woven cross-ply carbon/epoxy composite. Failure mechanisms including compression and buckling were observed and the ultimate strength of the component under compression was significantly less than that of the material.

KEYWORDS: carbon/epoxy composite, suspension push-rod, Formula 1, compression, fracture, buckling.

1 INTRODUCTION

A central load-bearing structure in a modern F1 car connects the front and rear suspension systems; this load-bearing structure consists of the monocoque, the engine and the gearbox casing. The driver, fuel tank and front suspension dampers are housed within the monocoque whilst the engine is jointed to the back of the monocoque on four studs. The gearbox casing is attached to the rear face of the engine. This three-piece box-beam structure carries the inertial loads to the four corners of the car. Various wing structures, underbodies, cooler ducting and bodywork are attached to and around this box-beam.

More than 80% of a modern Formula 1 car is made from some form of composite material, with the majority being based on carbon/epoxy systems. Such extensive use originates back to the mid-1970s when the “wing-car”, developed by Lotus, created large downforce by using the underneath of the car. This required large wing-shaped underbodies to be attached to a chassis of reduced width, the torsional rigidity of which could only be maintained efficiently by use of composite materials. Additionally, turbochargers emerged in the late 1970s and, producing in excess of 1400 bhp, these led to severe loads being applied to the chassis. Composite materials offered greater specific stiffnesses and greater flexibility in design than the aluminium alloys that had been used previously.

In 1981 the monocoque of the McLaren MP4 F1 car was first moulded from a carbon fibre reinforced epoxy polymer. The monocoque was moulded over a machined aluminium tool which was subsequently removed in sections through the cockpit opening. Unidirectional carbon/epoxy was used for the skins whilst aluminium honeycomb was used for the core. This design was used virtually unchanged for six racing seasons, so successful was the one-piece construction. A two-piece construction was pioneered by Gustav Brunner in 1983 for his ATS F1 car by moulding the monocoque as top and bottom halves in a female mould. This had advantages of providing greater flexibility in the geometry and size of the monocoque over the one-piece construction.

More recently, however, composites have begun to be used in manufacturing components other than primary structural parts, such as, for example, high-strength components, the gearbox casing, where torsional rigidity is crucial, and suspension components, which require high stiffness. Traditional metal suspension components are being replaced by composites in order to increase the stiffness of the individual suspension members, and thereby give the designer more control over the overall stiffness of the suspension system. It is the push-rod which has the single major influence on the stiffness of the suspension system. However, the change from metal to composite components has not been without

problems for many F1 teams. Williams, for example, replaced the metal push-rod by a composite push-rod but had to revert to the metal component due to a series of rear suspension failures in testing.

This particular paper aims to investigate the performance of a composite push-rod under compression which should consequently assist design engineers to predict the ultimate limits to which a composite push-rod can be used. The geometry and stacking sequence that were used to manufacture the push-rods are discussed, as is the experimental test setup that was used to apply direct compression to the components. The performance of the push-rods under compression, the manner of failure and the fracture mechanisms that were observed are discussed.

2 PUSH-ROD DESIGN & MANUFACTURE

2.1 Geometry and stacking sequence

In order to minimise the effects of wind-drag around the push-rods it was decided to utilise an aerofoil cross-section instead of a circular cross-section. Uniform and tapered layups were used, the purpose of the taper being to increase the equivalent modulus along the critical section of the push-rod and consequently, to increase the load at which buckling would occur. Since the end sections of both the tapered and uniform layups were identical it was anticipated that the load at which compression failure should occur would be identical for both types of push-rod. The push-rod was 650mm long whilst the nominal wall thickness was 1.825mm for the uniform push-rod and varied between 1.825-2.450mm for the tapered push-rods. The external major and minor dimensions of the airfoil axes were nominally specified at 38mm x 18mm.

One objective of this project was to investigate the influence of the lay-up on the possible buckling response of the push-rod. Since the principal in-service mechanical load on the push-rod was uniaxial compression, it was necessary to maximise the number of 0° plies within the stacking sequence in order to provide maximum uniaxial stiffness. A number of cross-ply plies were necessary, however, to prevent longitudinal splitting of the push-rod. The first stacking sequence that was considered was a uniform layup of (0°/90°,0°,0°/90°), i.e., two external 0°/90° cross-ply plies of woven prepreg surrounding nine

unidirectional 0° plies. This layup differs from that which is typically used in current F1 design only in that there are no tapered plies within the stacking sequence. As such, it was anticipated that the ultimate mechanical response of this push-rod design would be a lower bound limit and failure would be due to buckling.

The remaining two push-rods were identically tapered centrally along their mid-lengths and the particular stacking sequence that was used was (0°/90°,0°₇,90°,0°₆,0°/90°), i.e., two outer 0°/90° cross-ply plies of woven prepreg surrounding seven 0° plies, one 90° ply and six 0° plies. The taper was obtained by only placing some of the 0° and 90° plies along part of the 650mm length of the push-rods.

Commercially available laminate analysis software was used (LAP, 1991) to estimate the equivalent laminate properties (shown in Table 1) from the precise ply properties of Table 2.

Table 1. Equivalent mechanical properties of uniform and tapered layups used to manufacture the different push-rods.

Equivalent laminate property	Uniform Layup	Tapered Layup
E_{xx} , [GPa]	211	221
E_{yy} , [GPa]	23.7	34.7
ν_{xy}	0.115	0.068
ν_{yx}	0.013	0.011
G_{xy} , [MPa]	11.6	11.7

Table 2. Mechanical properties of the 0°/90° woven and unidirectional carbon/epoxy material systems used to manufacture the composite push-rods.

Mechanical property	0°/90° woven ply	unidirectional ply
Thickness	0.35mm	0.125mm
Longitudinal stiffness	53GPa	310GPa
Transverse stiffness	52GPa	5.9GPa
Shear modulus	0.011GPa	0.012GPa
Poisson's ratio	0.1	0.2
Longitudinal tensile strength	690MPa	1960MPa
Longitudinal compressive strength	59MPa	700MPa
Transverse tensile strength	690MPa	354MPa
Transverse compressive strength	59MPa	354MPa
Shear strength	80MPa	100MPa

2.2 *Manufacture of Push-rods*

Three separate carbon/epoxy push-rods were manufactured by wrapping the various plies of prepreg around a hollow elliptical silicone mandrel. This was then placed within an elliptical two-part cavity mould and cured in an autoclave. The hollow mandrel acted as an expandable bladder during the curing cycle, thereby pressing the prepreg firmly against the walls of the mould and ensuring that a uniform wall thickness was produced along the length of the push-rod.

The autoclave curing cycle for the woven and unidirectional carbon/epoxy prepreg involved a 90 minutes cure at 125°C and 700kPa with a heat-up and cool-down rate of 2.3°C per minute. When the temperature reached 125°C the vacuum was vented to atmosphere. Pressure was then introduced and ramped at 50kPa per minute to 700kPa. When the pressure cycle was completed the pressure was ramped down at 50kPa per minute to 0kPa, at which stage the vacuum was reintroduced.

Both the mould and the silicone mandrel were reused when manufacturing all three push-rods and these were cleaned and degreased before being coated with release agent (FreeKote) prior to the plies of carbon/epoxy prepreg being wrapped around the mandrel and placed within the mould. The complete assembly was vacuum bagged to evacuate air, solvents and entrapped volatiles from the laminate and to allow the positive autoclave pressure to consolidate the laminate against the mould surface. A breather cloth bagging assembly was used to absorb any excess resin flow and also to smooth out the sharp corners of the mould, which could cause the vacuum bag to rupture under the high autoclave pressures. A solid release film was placed against the mould walls to prevent the breather cloth from sticking to the mould surfaces.

Upon completion of the curing cycle, the vacuum bag assembly was removed from the autoclave. The bag and breather were discarded and the end plates were removed prior to the mould being opened. The composite push-rod was then taken from the mould and the silicone mandrel removed from the centre of the push-rod.

Before the actual carbon/epoxy push-rods could be manufactured, it was necessary to manufacture a suitable elliptical mould and elliptical silicone mandrel so that the finished push-rods would be of the required thickness and cross-

section. The mould was machined from aluminium whilst the silicone mandrel was manufactured using GFRP slips, an elliptical copper pipe and the mould. The copper pipe was located centrally within the mould cavity through an aluminium end-plate. The end-plate was subsequently bolted to the mould and the mould was inverted. The GFRP slips were placed against the mould walls and de-aerated liquid silicone rubber was poured into the space between the GFRP slips and the copper pipe in the mould. This assembly was left under room conditions for fourteen hours to allow the rubber compound to cure and was then placed in an oven at 120°C for 90 minutes to complete the curing process. The hollow silicone mandrel was then removed from the mould and the copper pipe was extracted from the mandrel. No significant air bubbles or voids, which would have made the mandrel unsuitable for manufacturing the push-rods, were detected visually.

The GFRP slips were fabricated using the two halves of the mould. After spraying release agent on both halves of the mould, six plies of GFRP were stacked in each half of the mould. The two halves of the mould were covered in a release ply, covered with a bleeder cloth and placed in a vacuum bag, which was then sealed. The assembly was cured in the autoclave using an appropriate cycle.

A fourth carbon/epoxy push-rod was manufactured using a sand-bag technique instead of the silicone mandrel, which ruptured when being removed from the third push-rod. The procedure involved in making this core used a cylindrical nylon tube (thermally stable, thin and impermeable). The mould, with the GFRP slips, was then bolted together and the nylon tube was inserted into the mould cavity. The tube was sealed at one end using sealant tape and dry sand was then added to the tube and compacted by means of a vacuum pump. The subsequent procedure for manufacturing this fourth push-rod was identical to that based on using the silicone mandrel.

However, this fourth push-rod was laid up incorrectly with a slight overlap in the first ply, which prevented the first ply from expanding and consolidating against the other plies in the mould during the autoclaving process. This prevented resin from flowing to the surface and consequently exposed fibres were detected at the outer surface of the push-rod after manufacture. In normal operating conditions such a component would be scrapped. Nevertheless, this push-rod was tested in the same manner as the other three push-rods and the results

of this test is also discussed in the following sections.

3 EXPERIMENTAL TEST PROCEDURE

Four push-rods have been tested statically to failure under compression using a displacement mode of control on a 100kN uniaxial servohydraulic fatigue machine (Series 8501 Instron). The loading was introduced at both ends of a push-rod using female end-fixtures which had been designed to provide boundary conditions that were pin-jointed at the bottom and cantilevered at the top in order to simulate in-service support conditions.

Surface strains, from gauges at three different positions on the push-rods, were recorded using a data acquisition system which operated on a keypress sequence. Strain gauges were aligned longitudinally and transversely along the length of the push-rods to measure the performance under compressive load. Two gauges were aligned axially at the midlength and opposite faces of the push-rods: these provided information on the presence of buckling, the deviation from linearity in the mechanical response of the push-rod and fracture strains. A third strain gauge was aligned normal to the first two gauges and was used to calculate values of Poisson's ratio.

4 BEHAVIOUR OF PUSH-RODS UNDER COMPRESSIVE LOADING

All push-rods were loaded statically to failure by means of a displacement mode of control. Load, displacement and strain values were collated at increments of actuator load. As the applied load was increased from zero, the response of the push-rods was initially linear elastic. Figures 1-4 detail the variation of compressive surface strains at the mid-length position on opposite sides of the four push-rods with increasing actuator load. The strain responses deviated from linearity at approximately 90% of the final failure load although minor fracture events occurred before this deviation from linearity in the first and fourth push-rod tests (at 10.8kN in Figure 1 and 18.75kN in Figure 4, respectively). This deviation of the strain difference (i.e., magnitude of strain difference between front and back faces of the push-rods) from linearity, which occurred at approximately 90% of the final failure load identified the onset of catastrophic fracture.

Ultimate failure of the first uniformly laid-up push-rod occurred some 40mm from the centre of the specimen whilst failure of the remaining three push-rods was concentrated around the the pin-jointed end-fixture of the testing machine. Table 3 summarises the loads and strains at which ultimate failure occurred during the four tests.

Table 3. Summary of ultimate actuator loads, surface strains and compressive failure locations.

Specimen	Load	Strain	Location
Push-rod 1	31.00k N	0.182%	40mm from centre
Push-rod 2	30.00k N	0.160%	pin-joint end
Push-rod 3	30.25k N	0.111%	pin-joint end
Push-rod 4	28.75k N	0.104%	pin-joint end

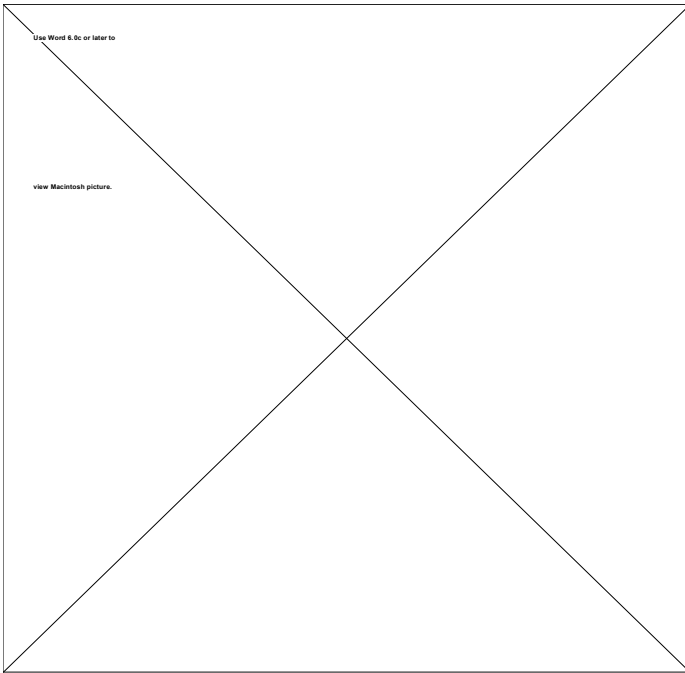


Figure 1. Variation of surface strains with actuator load during testing of push-rod 1. Buckling is identified by the difference between the values of the two surface strain readings and begins with the onset of actuator load. Incipient fracture begins at approximately 26kN.

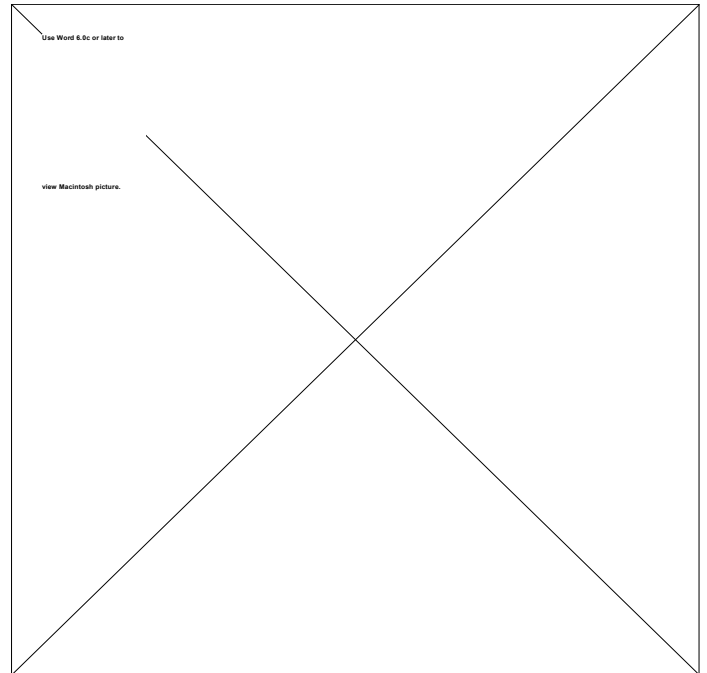


Figure 3. Variation of surface strains with actuator load during testing of push-rod 3. Buckling is identified by the difference between the values of the two surface strain readings and begins with the onset of actuator load. Incipient fracture begins at approximately 29kN.

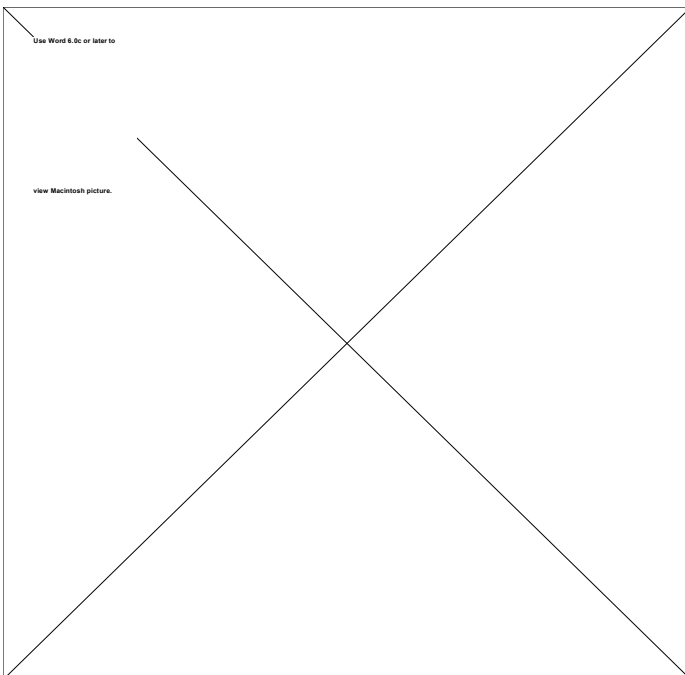


Figure 2. Variation of surface strains with actuator load during testing of push-rod 2. Buckling is identified by the difference between the values of the two surface strain readings and begins with the onset of actuator load. Incipient fracture begins at approximately 28kN.

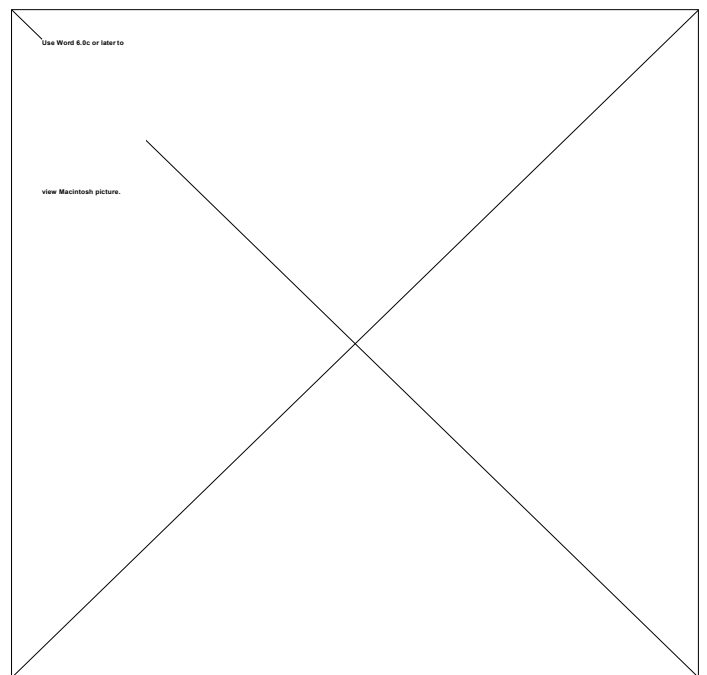


Figure 4. Variation of surface strains with actuator load during testing of push-rod 4. Buckling is identified by the difference between the values of the two surface strain readings and begins with the onset of actuator load. Incipient fracture begins at approximately 28kN.

The measured actuator loads and surface strains are presented in Figures 1-4 for the four push-rods. The average load-strain relationship for all the push-rods is essentially linear almost until fracture. However, the individual strain-gauge readings deviate from linearity immediately with the application of load and this deviation continues to increase directly with applied load up until failure.

Table 3 identifies the maximum direct compressive strains which were measured during each test and may be compared against the failure strains of the carbon-fibres of 1.5% (Lovell, 1991). While the maximum direct strain reading at failure of push-rod 1 (i.e., 0.18%) is greater than those recorded during the other three tests (this is to be expected since the strain gauge position of this push-rod was closer to the failure site than in all other tests), this is considerably less than the fibre failure strain. Consequently, failure of these components is due to geometric and manufacturing limitations rather than material limitations.

4.1 *Buckling Behaviour*

A simple first mode of buckling was apparent along the length of the four test specimens, with maximum lateral deformation (i.e., crest of the buckle) occurring close to the mid-length of the push-rods. Buckling initiated with the application of load in all push-rod tests, as can be seen from the deviation of the two sets of surface strain gauge readings (Figures 1-4) from the average compressive strain. The amplitude of the buckle increased linearly in size with actuator load until failure. No dial gauges were used during the tests to quantify the amplitude of the buckle although this could be estimated from the degree of curvature and bending that has been measured by the surface strain gauges.

4.2 *Damage in Push-rods*

The compressive failure mechanisms that occurred in all four push-rods were similar although failure of push-rod 1 occurred at a position close to the mid-length of the component whereas failure was close to the pin-jointed end for the other three push-rods. The reason for this different failure site is due to the fact that push-rod 1 was manufactured without any tapered region in its mid-section, unlike the other three push-rods. The general appearance of the fracture associated with push-rod 4 is shown in

Figure 5. The appearance of the fracture surface is different both around the perimeter of the push-rod and through the thickness of the push-rod. The fracture is not uniformly compressive around the perimeter and this is due to the differential buckling strains that existed on opposite sides of the push-rod. The lack of similarity of the through-thickness fracture features is partly due to the variation of compressive strains and partly due to the different ply orientations through the thickness of the push-rod.

Figure 5. Compressive fracture of push-rod 4 as identified visually. The outer 0°/90° woven ply is clearly visible. The damage mechanism that initiated failure was due to compressive stress (near side in photograph).

Figures 6 and 7 detail the initiating compressive failure sites that led to ultimate fracture of the push-rods using scanning electron microscopy. Many broken fibres are evident in Figure 6 and the manner in which these fibres fractured is characteristic of compressive failure, i.e., fibre microbuckling and localised fibre fracture (Gilchrist et al., 1996a, b).

Buckling occurred in all cases and this increased directly with the application of load. The ultimate performance of these particular push-rods was limited by geometric, manufacturing and support parameters and was not close to the ultimate fibre failure strains of the materials that were used.

ACKNOWLEDGEMENTS

Financial support in the form of a President's Research Award from University College Dublin is gratefully acknowledged. The authors are happy to express their gratitude to Jordan's Formula 1 for providing composite prepreg materials.

REFERENCES

- Gilchrist, M. D., Kinloch, A. J., Matthews, F. L. & Osiyemi, S. O., 1996a, Mechanical performance of carbon fibre and glass fibre-reinforced epoxy I-beams: I - Mechanical behaviour. *Composites Science & Technology*, 56, pp. 37-53.
- Gilchrist, M. D., Kinloch, A. J. & Matthews, F. L., 1996b, Mechanical performance of carbon-fibre and glass-fibre reinforced epoxy I-beams: II - Fractographic failure observations. *Composites Science & Technology*, 56, pp. 1031-45.
- LAP, 1991, *Laminate Analysis Program*, Centre for Composite Materials, Imperial College, London SW7 2BY, UK.
- D. R. Lovell, 1991, *Carbon & high performance fibres directory*, Edition 5, Chapman & Hall.

Figure 6. Micrograph of compressive fracture of push-rod.

Figure 7. Detailed micrograph of fractured fibres due to compressive failure of push-rod.

5 CONCLUSIONS

Unidirectional and woven cross-ply carbon/epoxy composites were used to manufacture suspension push-rods that could typically be used in a Formula 1 racing car. These were subsequently loaded to failure under compression using cantilevered and pin-jointed end supports. Three push-rods had a tapered mid section consisting of 0° and 90° plies whilst an initial trial specimen was of constant thickness along its length. Fracture of the trial specimen (push-rod 1) occurred close to the mid-length whilst fracture in all other cases was close to the pin-jointed support in the loading frame.